MICROWAVE FIELD MEASUREMENT OF NEW ZEALAND ALPINE SNOW WETNESS

Adrian E.-C. Tan[1], *Wolfgang Rack*[2], *Kimberley W. Eccleston*[1], *Ian G. Platt*[1], *E.-M. Anton*[1], *Ian M. Woodhead*[1]

1- Lincoln Agritech Ltd., Lincoln University, Christchurch, New Zealand
2- Gateway Antarctica, University of Canterbury, Christchurch, New Zealand

ABSTRACT

We present a method of measuring the complex permittivity of alpine snow in the microwave S-band (2.1-4 GHz) using the waveguide method. This method was field trialed in the Southern Alps in New Zealand, where six snow samples of varying melt conditions were measured and their complex permittivity calculated. Combined with snow density data, we estimated the volumetric liquid water content (i.e. snow wetness) of the snow samples. This data allows us to assess the viability of aerial snow depth surveys with the ultra-wideband radar.

Index Terms— snow wetness, volumetric water content, complex permittivity, waveguide measurements, field measurement.

1. INTRODUCTION

The objective of this study is to measure the liquid water present in pores of the frozen snow, called volumetric liquid water content, or snow wetness. Presence of liquid water in warm alpine snow attenuates microwave signals, limiting the performance of aerial surveys using microwave methods.

Aerial surveys of alpine snow provide an estimation of snowpack volume and coverage over a period of time, which is important to model the water cycle in alpine regions [1]. Conducting such estimation, however, is challenging due to weather variability, complex terrain and the presence of different land cover [2]. Typically, the snow water equivalent (SWE) of snow is estimated, which is used by hydrologists to assess the quantity of available water, model the water cycle, and conduct fresh water management [3]. Methods of estimating the SWE include in-situ measurements, remote passive microwave sensing, and remote active microwave sensing [4]. In-situ measurements like the snow pillow [5], the MagnaProbe [6] and the radio isotope snow gauges [7] provide relatively accurate point measurements of snow depths and SWE.

Remote passive microwave sensing measures the attenuation of microwave radiation emitted (brightness temperature) from the ground surface [8]. Remote active microwave sensing transmits an incident microwave signal onto the snow layer, measures the scattered signal and infer snow parameters from the properties of the signal [9]. The majority of work in the remote active microwave sensing involves space borne synthetic aperture (SAR) radars that operate in the C- and X-bands [10]. The ultra-wideband (UWB) radar is a non-satellite based remote active microwave sensing technique [11]. The UWB radar is usually deployed with aerial vehicles, flying over and surveying snow covered areas [12, 13].

The UWB radar utilizes signals that have very large bandwidths, thus allowing the radar to resolve targets at very high resolutions [14, 15]. Shown to be able to measure down to 2 m depths of cool, dry snow on sea ice in Antarctica, the UWB radar technique, however, faces significant challenges with warm wet snow where the presence of moisture attenuates the microwave signal as it propagates through the snow. This challenge forms the basis of this investigation – to develop a method of measuring the snow's complex permittivity and snow wetness in the field. The waveguide method has been used in Antarctica to measure cold snow on sea ice [12]. Other methods of snow dielectric permittivity measurements include the metallic snow fork [16], coaxial resonator [17], capacitive sensor [18] and ground penetrating radar [19]. A description of the waveguide measurement technique is presented in Section 2. The field measurement of warm alpine snow in New Zealand is described next, in Section 3. Measurement results and an analysis of the potential performance of the snow radar is presented in Section 4.

2. WAVEGUIDE MEASUREMENT OF SNOW

Consider a snow-filled WR284 rectangular waveguide section of length l operating in the TE_{10} mode (Fig. 1). The relative permittivity of snow, $\varepsilon' - j\varepsilon''$, is related to the propagation constant of the snow, k_{sn}, as

$$\varepsilon' - j\varepsilon'' = \left(\frac{k_{sn}}{k_0}\right)^2 \tag{1}$$

where $k_0 = 2\pi/\lambda$ is the propagation constant of a plane wave of wavelength λ. When expressed in the Cartesian coordinate system,

$$k_{sn}^2 = k_x^2 + k_y^2 + k_z^2 = \left(\frac{\pi}{a}\right)^2 + k_z^2 \tag{2}$$

for TE_{10} mode operation, where a (= 72.1 mm) is the larger dimension of the WR284 rectangular waveguide cross-section, and k_z is the z-component of k_{sn}. In terms of S_{21} parameter, the section of snow-filled waveguide in Fig. 1 can be expressed as

$$S_{21} = e^{-\alpha l - j\beta l} = e^{-jk_z l} \quad (3)$$

where $e^{-\alpha l}$ and $e^{-j\beta l}$ are the real and imaginary parts of the S_{21} parameter, and l is the length of the waveguide section. From (3), k_z can be calculated from the measured S_{21} of the snow-filled waveguide, and the relative permittivity of snow can be calculated with (1) and (2).

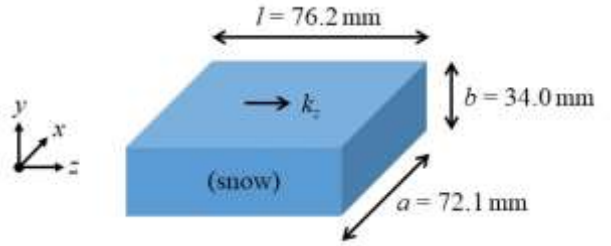

Fig. 1. A snow-filled WR284 rectangular waveguide section with waves propagating in the k_z direction in the TE_{10} mode.

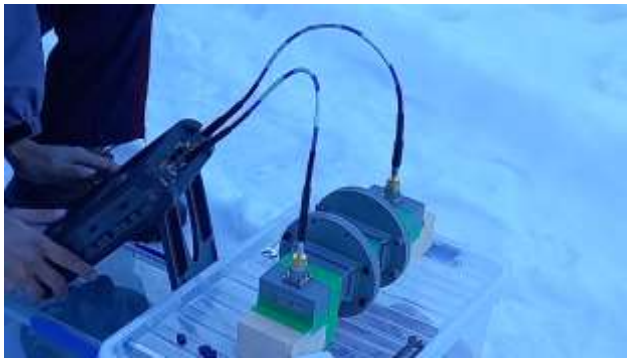

Fig. 2. Measurement setup where the two ports of the snow-filled waveguide section is connected to the vector network analyser via adaptors and coaxial cables.

In an actual *S*-parameter measurement, however, the snow-filled waveguide section is connected to ports 1 and 2 of the vector network analyser (Keysight Fieldfox N9923A) via coaxial-to-waveguide adaptors and coaxial cables, as shown in Fig. 2. In addition, to facilitate the extraction of snow sample and placement in the waveguide section, an open-ended plastic sample holder (3D printed) of dimensions 75 mm x 72 mm x 34 mm is used. The 2-port *S*-parameters (including S_{21} parameters used in (3)) of the waveguide section is calculated from measured 2-port *S*-parameters using the through-line de-embedding method [20].

3. FIELD MEASUREMENT OF ALPINE SNOW

A field measurement of alpine snow was conducted at the Broken River ski field (Arthur's Pass, New Zealand) on 28 May 2022. A snowfall event occurred two days prior, and the weather during the field measurement was clear sky with ambient temperature at 0 deg. Celsius. Six snow samples were collected from four snow pits (A, B, C and D) and were measured using the waveguide method. The snow pits were selected to cover a variety of snow conditions that were present in late autumn.

Snow pits A and B were shaded by trees, and had a single snow layer of 8 cm and 18 cm over unfrozen ground respectively. Snow pits C and D were exposed to the sun. Snow pit C consisted of two distinct snow layers, with the upper snow layer (5 cm) being coarse grained (3 mm) and slightly melting, while the lower snow layer (8 cm) being fine grained (< 0.5 mm). Snow pit D consisted of two snow layers underneath 1 cm of refrozen ice crust, with the upper layer (14.6 cm) being crusty snow, while the lower layer being soft snow. Fig. 3 shows an example microwave field measurement of snow (upper layer, snow pit C), where the snow sample is inserted into the waveguide section before being measured.

Fig. 3. Microwave waveguide measurement of snow in the field with snow sample, extracted using an open ended plastic sample holder, is inserted into the waveguide section.

4. RESULT AND ANALYSIS

Fig. 4 shows the complex permittivity of the six collected snow samples – The ε' values are fairly constant across the measured frequency range, and vary between 1.5 (Fig. 4d) and 1.8 (Fig. 4c) for different snow samples. ε'' values are small, varying between 0.0 and 0.17 for all samples, appear noisy and exhibit ripples. The apparent noise in ε'', when compared with ε' trace, is due to different *y*-axis scales. We confirmed this by estimating the signal noise of both ε' and ε'' data using the windowing method [21], and found that their noise levels are comparable. Further analysis also showed that, though more evident in ε'' plots in Fig. 4, ripples are present in both ε' and ε'' data. We attribute these ripples to imperfect field measurement conditions such as post-calibration instrument drift and coaxial cable flexure between calibration and snow measurements. To arrive at an estimate of ε'', we average the measured ε'' values across the frequency range of 2.3-3.8 GHz. The six snow samples are labelled (a)

to (f) in the 1st column in Table I, while their measured snow density data and averaged complex permittivity data are shown in the 2nd and 3rd columns respectively.

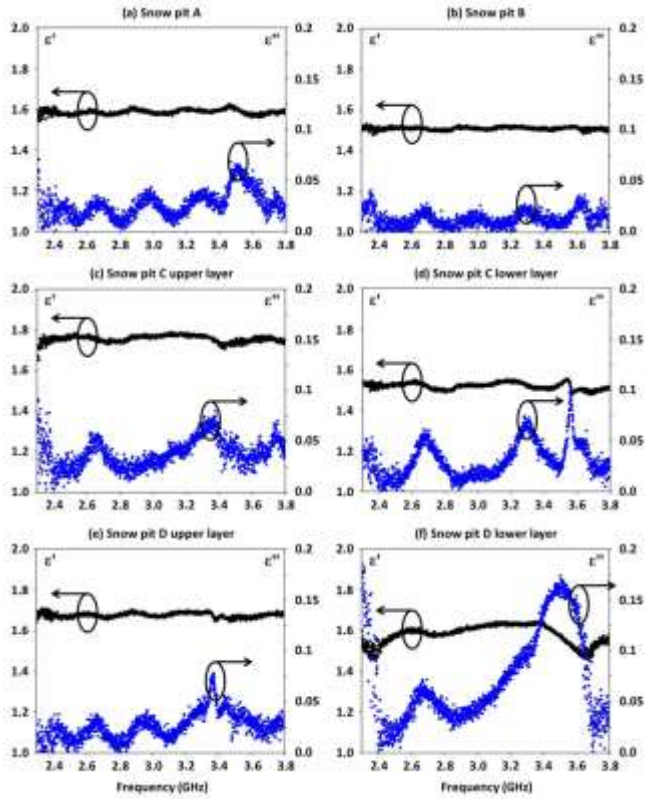

Fig. 4. Complex permittivity of six snow samples that were extracted from the snow pits are shown in subplots (a) to (f). ε' is plotted in black, while ε'' is plotted in blue.

TABLE I
MEASURED SNOW PARAMETERS

ID	Snow density (kg/m^3)	Complex permittivity	Vol. water content	In-situ snow observations
a	192	1.59 - *j*0.028	1.0 %	fresh powder snow
b	270	1.51 - *j*0.012	0.4 %	fresh snow
c	233	1.76 - *j*0.046	2.3 %	slightly melting
d	213	1.52 - *j*0.035	1.3 %	-
e	228	1.68 - *j*0.034	1.1 %	crusty with 1 cm ice layer above
f	218	1.63 - *j*0.094	2.6 %	soft, melting

Using the empirical snow model in [22], the volumetric liquid water content of snow is estimated from the snow density and complex permittivity data, and is shown in the 4th column. Comparison between the estimated volumetric water content (VMC) of snow with in-situ observations shows a good correspondence. For instance, samples (a) and (b) were fresh snow collected in shaded locations and both samples show the lowest ε'' values and VMC at 0.4 % and 1.0 % respectively; Samples (c) and (f) were exposed to sun, and are observed to be melting. In the measured data, they exhibit the highest ε'' values, and VMC at 2.3 % and 2.6 % respectively.

Having high quality data on snow wetness allows us to assess the viability of aerial snow surveys, keeping in mind the primary concern around reduced depth performance due to increased signal attenuation. In order for the radar to detect the second snow / ground reflection, the signal has to propagate through the snow layer twice. The presence of water in the snow attenuates the signal to a level that may render the reflections from sub-surface interfaces to be undetectable. Using the measured permittivity data of warm alpine snow, we can now better model the attenuation introduced by the presence of liquid water content in the snow, and thus are able to assess the snow radar's performance in aerial snow surveys.

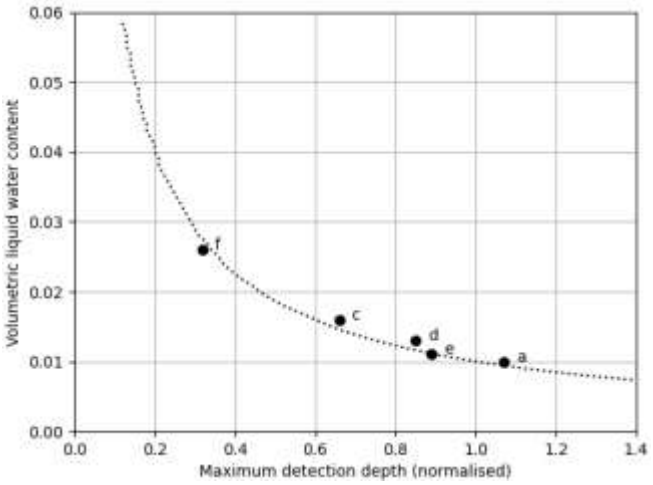

Fig. 5. Assessment of radar's detection of snow/ground reflection under a uniform snow layer of different volumetric liquid water content (VMC). The black dotted line shows the detection depth normalised to snow with a density of 250 kg/m^3 and volumetric liquid water content of 0.01. Labelled black circles indicate the radar's detection depth for the field measured snow samples.

Fig. 5 shows an assessment of the snow radar's ability to detect the snow/ground reflection that is buried under a uniform layer of snow of different volumetric liquid water content (VMC), assuming plane wave propagation in the snow layer. The black dotted line in Fig. 5 shows the detection depth of the snow radar, normalised to snow with density of 250 kg/m^3 and VMC of 0.01. From the dotted line, we can see that as the VMC increases from 0.01 to 0.02, the maximum detection depth of the snow radar reduces by a factor of 0.45, and for a VMC of 0.04, the maximum detection depth is reduced by a factor of 0.2. Using the same assessment method, the maximum detectable depth of the snow conditions measured during the field trial can be determined. The maximum detectable depth of five measured snow samples (a, c, d, e and f in Table 1) are plotted as black dots in Fig. 5. Snow sample (b) is not plotted because, having very

low VMC, its maximum detection depth is much higher (2.5 m), and is beyond the range of the figure.

5. CONCLUSION

We presented a waveguide method of measuring the complex permittivity of alpine snow. Using this method in field measurements, we were able to measure the permittivity and volumetric liquid water content of snow samples. Comparison between measured data and in-situ observations showed a good correspondence. Measured result from this trial indicate that snow radar aerial surveys of wet snow has good potential. Further field trials of the snow radar are required to better understand its performance for different ground and snow conditions.

6. REFERENCES

[1] J. Helmert *et al.*, "Review of Snow Data Assimilation Methods for Hydrological, Land Surface, Meteorological and Climate Models: Results from a COST HarmoSnow Survey," *Geosciences* vol. 8, MDPI, pp. 489, 14 December 2018.

[2] M. Taheri, and A. Mohammadian, "An Overview of Snow Water Equivalent: Methods, Challenges and Future Outlook," *Sustainability* vol. 14, MDPI, Switzerland, pp. 11395, 11 September 2022.

[3] P. Henkel *et al.*, "Snow Water Equivalent of Dry Snow Derived From GNSS Carrier Phases," *IEEE Trans. Geosci. Rem. Sens.*, vol. 56, no. 6, pp. 3561-3572, June 2018.

[4] S. Liang, and J. Wang, *Advanced Remote Sensing: Terrestrial Information Extraction and Applications*, Academic Press, Cambridge MA, 2019.

[5] J. Pflug, S. Margulis, and J. Lundquist, "Inferring Watershed-Scale Mean Snowfall Magnitude and Distribution using Multidecadal Snow Reanalysis Patterns and Snow Pillow Observations," *Hydrological Processes*, vol. 36, no. 6, Wiley Online Library, pp. e14581, 7 May 2022.

[6] M. Sturm, and J. Holmgren, "An Automatic Snow Depth Probe for Field Validation Campaigns," *Water Resource Research,* vol. 54, no. 11, Wiley Online Library, pp. 9695-9701, Nov 2008.

[7] C. Warnick, and V. Penton, "New Methods of Measuring Water Equivalent of Snow Pack for Automatic Recording at Remote Mountain Locations," *J. Hydrology*, vol. 13, Elsevier, pp. 201-215, 1971.

[8] L. Li, Y. Fan, H. Chen, and L. Zhan, "Sensitivity Analysis of Microwave Brightness Temperature to Snow Depth on Sea Ice in the Arctic," *IEEE International Geoscience and Remote Sensing Symposium*, Kuala Lumpur, Malaysia, 17-22 July 2022.

[9] R. Rincon, B. Osmanoglu, P. Racette, Q. Bonds, M. Perrine, L. Brucker, S. Seufert, and C. Kielbasa, "Tri-frequency Synthetic Aperture Radar for the Measurements of Snow Water Equivalent," *IEEE International Geoscience and Remote Sensing Symposium*, Yokohama, Japan, 28 July -2 August 2019.

[10] S. Leinss, O. Antropov, J. Vehviläinen, J. Lemmetyinen, I. Hajnsek, J. Praks, "Wet Snow Depth from Tandem-X Single-Pass Insar Dem Differencing," *IEEE International Geoscience and Remote Sensing Symposium*, Valencia, Spain, 22 -27 July 2018.

[11] A. Tan, J. McCulloch, W. Rack, I. Platt, and I. Woodhead, "Radar Measurements of Snow Depth Over Sea Ice on an Unmanned Aerial Vehicle," *IEEE Trans. Geosci. Rem. Sens.*, vol. 59, no. 3, pp. 1868-1875, March 2021.

[12] A. Tan, K. W. Eccleston, I. Platt, W. Rack, J. McCulloch, "Microwave Measurement of Snow over Sea-Ice in Antarctica," *International Conference on Electromagnetic Wave Interaction with Water and Moist Substances*, Lublin, Poland, 4-7 June 2018.

[13] A. Tan, J. McCulloch, W. Rack, I. Platt, and I. Woodhead, "Snow Depth Measurements from an Octo-copter Mounted Radar," *IEEE International Microwave Symposium*, Los Angeles, USA, 4-6 August 2020.

[14] H. Purdie, W. Rack, B. Anderson, T. Kerr, T. Chinn, I. Owens, and M. Linton, "The Impact of Extreme Summer Melt on Net Accumulation of an Avalanche Fed Glacier, as Determined by Ground-Penetrating Radar," *Geografiska Annaler: Series A, Physical Geography*, vol. 97, no .4, pp.779-791, November 2016.

[15] S. Gogineni, J. Yan, D. Gomez, F. Rodrigues-Morales, J. Paden, C. Leuschen, "Ultra-Wideband Radars for Remote Sensing of Snow and Ice," *IEEE International Microwave and RF Conference*, New Delhi, India, 14-16 December 2013.

[16] A. Sihvola, M. Tiuri, "Snow fork for field determination of the density and wetness profiles of a snow pack," *IEEE Trans. Geosci. Rem. Sens.*, vol. 24, no. 5, pp. 717-721, September 1986.

[17] C. Mätzler, "Microwave permittivity of dry snow," *IEEE Trans. Geosci. Rem. Sens.*, vol. 34, no. 2, pp. 573-581, March 1996.

[18] A. Denoth, "An electronic device for long-term snow wetness recording," Annals of Glaciology, vol. 19, pp. 104-106, 1994.

[19] J.H. Bradford, J.T. Harper, J. Brown, "Complex dielectric permittivity measurements from ground-penetrating radar data to estimate snow liquid water content in the pendular regime," *Water Resources Research*, vol. 45, W08403, 2009.

[20] K. W. Eccleston, "Verification of Extended Through-Line Deembedding," *IEEE Asia Pacific Microwave Conference*, Kuala Lumpur, Malaysia, 13-16 November 2017.

[21] E.C. Ifeachor, B.W. Jervis, *Digital Signal Processing – A Practical Approach*, Addison-Wesley, Harlow, England, ch. 10.

[22] M. Tiuri, A. Sihvola, E. Nyfors, M. Hallikaiken, "The Complex Dielectric Constant of Snow at Microwave Frequencies," *IEEE Journal of Oceanic Engineering*, vol. 9, no. 5, pp. 377-382, December 1984.